Vol. 600: 55–70, 2018
https://doi.org/10.3354/meps12634

MARINE ECOLOGY PROGRESS SERIES
Mar Ecol Prog Ser

Published July 30

Turbulent mixing and phytoplankton life history: a Lagrangian versus Eulerian model comparison

Jérémy Baudry[1], Dany Dumont[1,*], Irene R. Schloss[2,3,4]

[1]Institut des sciences de la mer de Rimouski (ISMER), Université du Québec à Rimouski (UQAR), Rimouski, Québec G5L 3A1, Canada

[2]Instituto Antártico Argentino, Buenos Aires, Argentina

[3]Centro Austral de Investigaciones Científicas (CADIC), CONICET, Argentina

[4]Universidad Nacional de Tierra del Fuego, Ushuaia, Argentina

ABSTRACT: Phytoplankton dynamics models follow either an Eulerian or a Lagrangian approach. The Eulerian formulation assumes that all individuals of a population living in homogeneous environmental conditions, i.e. within a model grid cell, are in a single average physiological state, which generally depends on local conditions. By tracking each individual cell or cluster of cells, the Lagrangian formulation allows population behaviour to emerge from a broader range of individual physiological states inherited from different life histories. In order to determine in which mixing conditions the widely used Eulerian approach differs from a more representative but also more computationally costly Lagrangian formulation, we compared the results obtained from a simple 1-dimensional phytoplankton growth model using both formulations under various mixing conditions. The chosen model is based on Droop kinetics, where growth is a function of light and an internal nutrient cell quota. It is applied in cases with constant and uniform diffusivity, and in more realistic cases of wind-induced and tidal mixing. The 2 main outcomes of our study are: (1) results from both formulations converge in weakly stratified environments for any level of turbulent mixing, and (2) results diverge in stratified environments and intermediate mixing up to a diffusivity value above which the environment appears homogeneous to moving cells, and both formulations converge. These results suggest that in heterogeneous and dynamic marine environments, strong variability among individuals may prevent Eulerian models from accurately predicting phytoplankton production.

KEY WORDS: Biogeochemistry · Individual Based Modelling · Population Based Modelling · Intrapopulation variability

INTRODUCTION

Biogeochemical modelling is widely used to study marine ecosystems and plankton dynamics. It is recognized as a powerful tool to study the behaviour of complex systems arising from basic underlying processes (Arhonditsis & Brett 2004). Most models mathematically represent biological processes as chemical reactions in which phytoplankton and other organisms are described in terms of concentrations rather than individuals. In this approach, hereafter referred to as the Eulerian approach (also known as 'lumped' models or population-level models), population dynamics are formulated using the so-called reaction-advection-diffusion equations (Franks 2002) in which dependent variables represent mean properties. Organisms are thus described as a continuum, and variability among individuals is not accounted for. However, a population of phytoplankton cells at a given time and location in its natural environment is composed of many individuals in different physiological states (Ross et al. 2011).

*Corresponding author: dany_dumont@uqar.ca

This intra-population variability generally results from the different life histories of individuals. In a turbulent environment, cells are randomly transported in the water column by eddies of various sizes. They thus experience different light and nutrient conditions along their respective trajectories. Additionally, they are able to adapt to the changing environment by modifying their biological response on time scales of less than one to several hours (Cullen & Lewis 1988). The reaction of a particular organism to its environment is thus intrinsically related to its trajectory in the water column, which determines its exposure to light and nutrients, and differs among individuals.

As our understanding of processes involved in the physiological response of organisms to their environment (e.g. photo-inhibition, photo-acclimation, nutrient uptake, respiration) has advanced significantly over the past decades, more adequate mechanistic and fully non-linear formulations of these processes have emerged in mathematical models (Baklouti et al. 2006). For example, classical Michaelis-Menten kinetics was gradually being superceded by Droop kinetics (Droop 1974), in which growth is decoupled from nutrient uptake, meaning that growth depends on an internal nutrient cell quota rather than on external nutrient concentrations. Nevertheless, adding these types of equations in the classical Eulerian paradigm remains fundamentally inaccurate (Woods & Onken 1982, Schuler 2005, Fredrick et al. 2013). As Bolnick et al. (2011) illustrated, the reason behind this inaccuracy is rooted in the so-called Jensen inequality (Jensen 1906), which states that 'averaging non-linear functions before integrating them is mathematically different than averaging the results of a non-linear integration'. In general, this implies that growth calculated by population-based models using average values of physiological parameters differs from the average growth calculated for each individual of the population. These arguments have motivated the development of alternative individual-based (or agent-based) models, here referred to as Lagrangian models, where populations are composed of a number of individual members whose locations are tracked and physiological states are integrated. Within this formulation, properties of a population are diagnosed and emerge from the collective behaviour of individuals. Over the past decades, the great potential of this approach has been recognized for phytoplankton ecology (Cianelli et al. 2012). Lagrangian models have been successfully applied to many issues such as competition dynamics (Huisman et al. 2004, Ross & Sharples 2007, Cianelli et al. 2009), photoresponses of cells to varying light (Kamykowski et al. 1994, Nagai et al. 2003, Esposito et al. 2009) or swimming strategies (Ross & Sharples 2008), and numerous standard protocols have been developed for the design of Lagrangian models (Ross & Sharples 2004, Grimm et al. 2006, Hellweger & Bucci 2009).

Several studies have attempted a comparison between Eulerian and Lagrangian formulations (e.g. Lande & Lewis 1989, Broekhuizen et al. 2003, Hellweger & Kianirad 2007). Hellweger & Kianirad (2007) studied a 1-dimensional test case where a continuous nutrient (phosphate) point source is advected into a straight river channel. They showed a difference of 30% in terms of total biomass between the Eulerian and Lagrangian formulations. However, they did not study the relation between turbulent mixing and the establishment of intra-population variability, which, in marine environments, is particularly important. To illustrate this, let us consider the case in which there is no mixing: all cells at a given location will be exposed to the same environment and will thus have the same life history. In this case, the intra-population variability is minimized and dynamics can be accurately represented using the classical Eulerian formulation. In contrast, in the case of strong vertical mixing in shallow waters whereby the water column is rapidly homogenized, gradients are minimized and all individuals have the same life history and could also be adequately simulated using an Eulerian approach. Between these extremes, there exists a wide range of mixing conditions leading to different individual dynamics. The question addressed here is then: Under what mixing conditions is it important to take into account individual life history? Also, what error are we making when we use a population-based Eulerian approach in such cases?

In this study, we examined the effect of turbulence on phytoplankton growth, expanding the study of Hellweger & Kianirad (2007) to marine systems by performing a systematic comparison between equivalent Eulerian and Lagrangian models under different vertical mixing conditions, ranging from idealized cases to more realistic ones. Phytoplankton growth is modelled following Droop internal nutrient quota kinetics. Below, we present the mathematical problem that we addressed, followed by a complete description of the model and the 2 formulations as well as the numerical experiments and model equivalence.

DEFINITION OF THE PROBLEM

Let us consider a group of phytoplankton cells moving in a turbulent environment. The population is sampled at a given time and depth, where environmental variables are homogeneous, and some physiological parameter X is measured n times so that we obtain a set of values $\mathbf{x} = x_1, x_2, ..., x_n$ of mean $\mathbb{E}[\mathbf{x}]$. Suppose that each phytoplankton cell has a growth rate that is a non-linear function of a particular parameter $f(\mathbf{x})$. In the Eulerian approach, the mean value $\mathbb{E}[\mathbf{x}]$ is used to parametrize the growth function, and the population's average growth rate is then computed as $f(\mathbb{E}[\mathbf{x}])$. However, Jensen's inequality theorem states that for a non-linear function $f(\mathbf{x})$, $f(\mathbb{E}[\mathbf{x}]) \neq \mathbb{E}[f(\mathbf{x})]$ (Jensen 1906).

An illustration of this inequality is provided by Hellweger & Kianirad (2007) in which they consider 2 sub-populations A and B with N:C ratio (nitrate cell quota) $Q_A = Q_0$ (see Table 1 for parameter specifications) and $Q_B = 3Q_0$, respectively. Let the growth rate be calculated using a Droop-type equation (Droop 1974) of the form $\mu = \mu_{max}(1 - Q_0/Q)$. In the Eulerian approach, the mean population-averaged cell quota is a state variable and would correspond to the average of the 2 sub-populations, which is $Q_{ave} = 2Q_0$. The corresponding growth rate is $\mu = 0.5\ \mu_{max}$. On the other hand, in the Lagrangian approach, the growth rate is first calculated for each sub-population $\mu_A = 0$, $\mu_B = 0.67\ \mu_{max}$ and the population-averaged growth rate is diagnosed, resulting in a lower value of $\mu = 0.33\ \mu_{max}$.

The heart of the problem is thus a mathematical one which arises from dealing with a non-linear biological process and on the physiological variability within a population: the larger the variability among individuals (larger spread of biological parameter values around the mean), and the stronger the non-linearity, the larger the difference between the Eulerian and Lagrangian solutions may become. Assuming that intra-population heterogeneity comes from the turbulent motion of the water that randomizes cells' trajectories and imposes different life histories to individual cells, we ask here in what way turbulent mixing affects how Lagrangian and Eulerian results differ. In other words, what kind of errors are we making when we model homogeneous instead of heterogeneous populations?

BIOLOGICAL MODEL DESCRIPTION

For the purpose of the study, the biological model is reduced to its simplest form, growth being only formulated as a function of light and nutrient uptake using a Droop-type model (Droop 1974). Although this model does not account for photo-acclimation and photo-inhibition, e.g. as in Ross & Geider (2009), it contains the proper amount of complexity needed to capture the underlying mechanisms responsible for intra-population variability with regards to nutrient uptake dynamics in the presence of vertical nutrient gradients generated by turbulence. This section presents the state equations used in the Eulerian and Lagrangian simulations.

Table 1. Model parameters. All parameters were chosen to be typical values and were not meant to represent a specific phytoplankton species. Conditions were set to represent a coastal area during summer. Sources: 1: Broekhuizen (1999), 2: Dortch & Maske (1982), 3: Sharples (1999), 4: Brand & Guillard (1981), –: this study

Symbol	Description	Value	Unit	Source
V_{max}	Maximum uptake rate	1	molN molC^{-1} d^{-1}	2
k_n	Half saturation constant	0:214	mmolN m^{-3}	1
k_e	Excretion rate	0.1	d^{-1}	–
δ	Respiration rate	0.1	d^{-1}	3
α^*	Photosynthetic growth rate constant	2.0	d^{-1}	2
α_{max}	Maximum photosynthetic growth rate	1.6	d^{-1}	2
Q_{min}	Subsistence cell quota	0.05	molN molC^{-1}	1
Q_{max}	Maximum storage quota	0.25	molN molC^{-1}	1
Δz	Resolution of the grid	0.5	m	–
Δt	Time step	6.0	s	–
ω_P	Phytoplankton settling velocity	0:2	m d^{-1}	–
H	Depth of the water column	40	m	–
I_s	Saturation onset constant	50	µE m^{-2} s^{-1}	4
k_d	Light attenuation constant	0.3	m^{-1}	–
N_0	Initial external nutrient concentration	5:0	mmolN m^{-3}	–
P_0	Initial particle biomass	4×10^{-6}	molC	–
Q_0	Initial cell quota	0.15	molN molC^{-1}	–

Eulerian formulation

In the Eulerian model, P and N are the 2 population state variables, respectively the phytoplankton concentration (molC m^{-3}) and the intracellular nutrient content (molC m^{-3}), and N_{ext} is the environmental nutrient concentration (molN m^{-3}). Their evolution is described by the following set of ordinary differential equations:

$$\frac{dP}{dt} = \mu P \quad (1)$$

$$\frac{dN}{dt} = (V - E)P \quad (2)$$

$$\frac{dN_{ext}}{dt} = (E - V)P \quad (3)$$

In Eq. (1), μ is the specific growth rate (d^{-1}) defined as $\mu = \alpha - \delta$, where δ is the constant respiration rate and α is the specific photosynthetic growth rate formulated as a Droop-type formulation based on a cell quota $Q = N/P$ (Droop 1974) with a single nutrient limitation, which is given by:

$$\alpha = \begin{cases} F\ \alpha^{\star}\left(1 - \frac{Q_{min}}{Q}\right) & \text{if } Q > Q_{min} \\ 0 & \text{if } Q \le Q_{min} \end{cases} \quad (4)$$

where $\alpha^{\star}$ is a constant parameter (d^{-1}) that controls the maximum specific photosynthesis rate, which depends on the subsistence cell quota Q_{min} and the maximum storage quota Q_{max}. If internal nutrients and light are not limiting ($Q = Q_{max}$ and $F = 1$), the growth rate reaches a maximum value $\alpha_{max} = \left(1 - \frac{Q_{min}}{Q_{max}}\right)\alpha^{\star}$. This means that for $Q_{min} = 0.05$ and $Q_{max} = 0.25$ molN $molC^{-1}$, the maximum specific photosynthetic growth rate is $\alpha_{max} = 0.8\alpha^{\star}$. The light limitation function F is a saturating response curve given by:

$$F(z) = 1 - \exp\left(-\frac{I(z)}{I_s}\right) \quad (5)$$

with I_s the saturation onset constant (μE m^{-2} s^{-1}). Following Ross & Sharples (2007), the specific uptake rate V of environmental nitrate by the cell is expressed using a saturating Monod function, mimicking Michaelis-Menten kinetics, given by:

$$V = V_{max}\left(1 - \frac{Q}{Q_{max}}\right)\frac{N_{ext}}{k_n + N_{ext}} \quad (6)$$

where V_{max} is the maximum specific uptake rate (molN $molC^{-1}$ d^{-1}) and k_n is the nutrient half-saturation constant (molN m^{-3}). Finally, $E = k_e Q$ is the excretion rate (molN $molC^{-1}$ d^{-1}), which is a function of the intracellular nutrient content, with k_e the excretion constant (d^{-1}). In the Eulerian model, the transport is computed using the advection-diffusion equation:

$$\frac{\partial C}{\partial t} = \frac{\partial}{\partial z}\left(K\frac{\partial C}{\partial z}\right) - w\frac{\partial C}{\partial z} \quad (7)$$

where C is substituted by P, N and N_{ext}, K is the turbulent diffusivity (m^2 s^{-1}), and w is the sinking velocity (m s^{-1}). Note that $w = 0$ for N_{ext} and $w = w_p$ (see Table 1 for parameter specifications) for P and N.

Lagrangian formulation

In the Lagrangian formulation, we solve for each particle i with biomass P_i and internal nitrate content N_i. The population state variables $\tilde{P}$ and $\tilde{N}$ as well as the environmental nutrient concentration $\tilde{N}_{ext}$ are diagnosed through integration over all particles within 1 grid cell of size $\Delta z = 0.5$ m. The evolution of a particle biomass is given by:

$$\frac{dP_i}{dt} = \mu_i P_i \quad (8)$$

where $\mu_i = \alpha_i - \delta$ and α_i is obtained from Eq. (1) using the value of the individual quota $Q_i = N_i/P_i$ instead of the population average quota $Q = N/P$. The index i is used for particles within 1 grid cell where environmental variables are homogeneous. Similarly, the evolution of the individual nitrate content N_i is given by:

$$\frac{dN_i}{dt} = (V_i - E_i)P_i \quad (9)$$

where V_i and E_i are obtained using Q_i.

In the Lagrangian model, particles living in a turbulent fluid are transported using a random walk algorithm (Hunter et al. 1993, Visser 1997, Ross & Sharples 2004) where the position of each particle z_{n+1} is related to its previous position z_n according to:

$$z_{n+1} = z_n - w\Delta t + K'(z_n)\Delta t + R\left[\frac{2K\left(z_n + \frac{1}{2}K'(z_n)\Delta t\right)\Delta t}{r}\right]^{1/2} \quad (10)$$

where z_{n+1} and z_n denote the vertical position of a particle respectively at time $n + 1$ and n, and $K'(z_n) = \partial K/\partial z$ evaluated at the vertical position z_n. Each particle moves randomly upward or downward at each time step Δt depending on R, which is a random process of 0 mean and variance r. The amplitude of the displacement depends on the value of the diffusivity K. Boundary conditions are set to satisfy:

$$z_{n+1} = \begin{cases} -z_{n+1} & \text{if } z_{n+1} < 0 \\ 2H - z_{n+1} & \text{if } z_{n+1} > H \end{cases} \quad (11)$$

where H is the water column depth. The environmental nutrient concentration in the Lagrangian model changes according to:

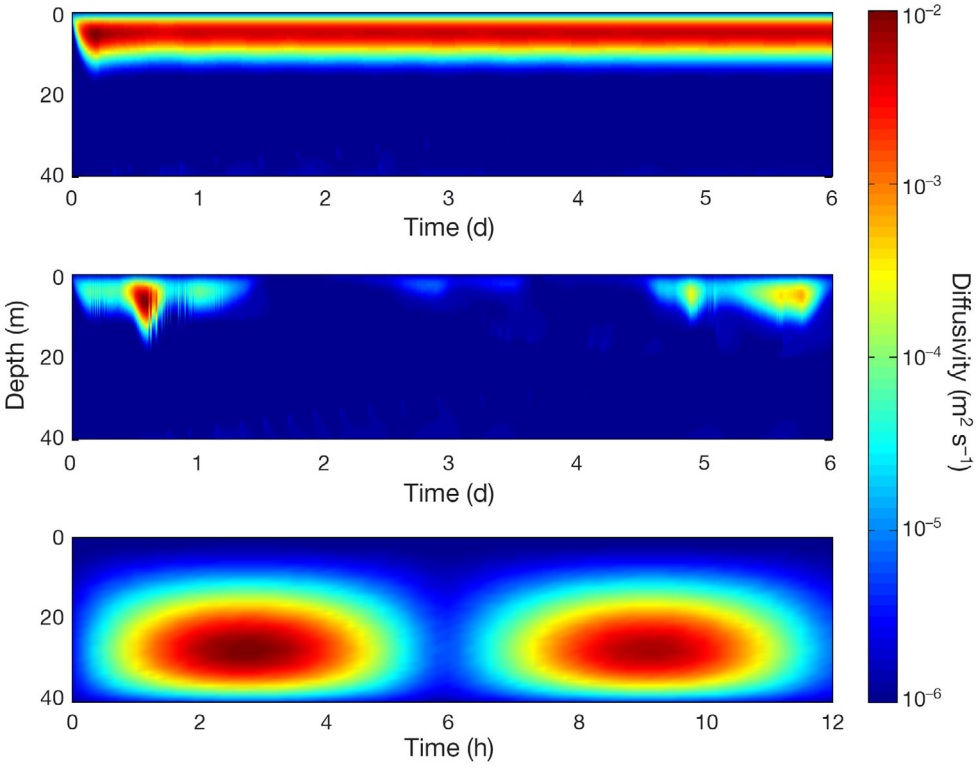

Fig. 1. Time evolution of the diffusivity profile used in experiments (a) K_5 (constant wind), (b) K_6 (variable wind) and (c) K_7 (barotropic M_2 tide with a mean current speed of 0.5 m s^{-1}). Note the different time scale in panel (c). See Table 2 for descriptions of the numerical experiments

$$\frac{\mathrm{d}\tilde{N}_{\mathrm{ext}}}{\mathrm{d}t} = \frac{1}{\Delta z}\sum_i (E_i - V_i)P_i \tag{12}$$

and is transported using the Eulerian advection-diffusion Eq. (7). In order to compare Lagrangian and Eulerian results, the population state variables and their corresponding evolution equations are calculated by summing over all particles. For phytoplankton and internal nutrient cell quotas, the mass balance equations are:

$$\frac{\mathrm{d}\tilde{P}}{\mathrm{d}t} = \frac{1}{\Delta z}\sum_i \mu_i P_i \tag{13}$$

$$\frac{\mathrm{d}\tilde{N}}{\mathrm{d}t} = \frac{1}{\Delta z}\sum_i (V_i - E_i)P_i. \tag{14}$$

NUMERICAL EXPERIMENTS

The characterization of the error between Eulerian and Lagrangian results follows a step-by-step approach where we define different mixing scenarios with increasing levels of realism. The first set of experiments uses uniform and homogeneous turbulent diffusivity profiles over a 40 m deep water column. In a second set of experiments, we use the *K*-profile parameterization turbulence model (Large & McWilliams 1994) and the General Ocean Turbulence Model (GOTM, Umlauf & Burchard 2005) to compute time-dependent diffusivity profiles produced by (1) constant and (2) varying surface wind stress, and (3) tidal mixing (Fig. 1). Details about the experiments are given in Table 2. In all experiments, we considered surface irradiance varying according to a semi-sinusoidal signal reproducing a 16 h day length, corresponding to the day length at mid-latitude during summer and peaking at noon at 1200 µE m^{-2} s^{-1}. Irradiance then decreases exponentially with depth according to the Beer-Lambert law:

$$I(z) = I_0 \exp(-k_{\mathrm{d}} z) \tag{15}$$

where I_0 is the surface irradiance and k_{d} is the light attenuation constant (m^{-1}).

Table 2. Description of numerical experiments

Experiment	Turbulent regime
K_1	Uniform $K = 1 \times 10^{-6}$ m^2 s^{-1}
K_2	Uniform $K = 1 \times 10^{-4}$ m^2 s^{-1}
K_3	Uniform $K = 1 \times 10^{-3}$ m^2 s^{-1}
K_4	Uniform $K = 1 \times 10^{-2}$ m^2 s^{-1}
K_5	Diffusivity profile produced by a constant wind of 8 m s^{-1}
K_6	Diffusivity profile produced by variable wind
K_7	Diffusivity profile produced by a barotropic M_2 tidal forcing mixing

Numerical aspects and stability

A major caveat of the Lagrangian formulation lies in the fact that only a limited number of particles can practically be tracked at a reasonable computing cost. On the other hand, an insufficient number of particles produces artificially noisy solutions, which would affect the accuracy of the results. The value of the time step Δt and the grid resolution Δz must also be chosen so that solutions are numerically stable. For Eulerian calculations, the first stability criterion is given by the diffusive Courant-Friedrich-Levy condition given by:

$$K \leq \frac{\Delta z^2}{\Delta t} \tag{16}$$

In the Lagrangian formulation, solving for the random walk requires that the diffusivity profile is both continuous and differentiable, which leads to the following second criterion (Ross & Sharples 2004):

$$\Delta t \ll \min\left|\frac{1}{K''}\right| \tag{17}$$

where $K'' = \partial^2 K/\partial z^2$. For all simulations a time step $\Delta t = 6$ s and a resolution $\Delta z = 0.5$ m were sufficient to meet the first criterion. In simulations with variable mixing, diffusivity profiles have been computed with a grid resolution of 1 m with GOTM and re-interpolated on the model grid, assuring that diffusivity profiles are sufficiently smooth to meet the second criterion. We set the number of particles to $N = 20\,000$, which corresponds to an average number of 250 particles per grid cell. Since the standard deviation of the numerical noise is proportional to $N^{-1/2}$ (Hunter et al. 1993, Graham & Moyeed 2002), this number is sufficient to produce accurate results.

Testing model equivalence

According to Hellweger & Kianirad (2007), the main difference between Eulerian and Lagrangian simulation results comes from the non-linearity of the problem. Therefore, if the particle growth is linearized, both models should produce the same results. Hellweger & Kianirad (2007) thus compared both models using linearized Monod equations and showed that in this case, Eulerian and Lagrangian formulations provided the same results. While that procedure was sufficient to verify their model implementation and avoid numerical bugs, it was not adequate to truly illustrate the consequences of Jensen's inequality. For example, Fig. 2a,b shows the results of Eulerian and Lagrangian models using the complete non-linear Monod equation. It appears that the 2 formulations give identical results (in the limit of large numbers of particles), showing that non-linearity is not solely responsible for differences between Eulerian and Lagrangian formulations. Non-linearity must affect cells differently, which is not the case in the Monod formulation where growth is a function of external nutrient intake. Thus, all individuals of a population at a given time and location have the same physiological response. However, in the Droop model, growth and nutrient uptake are decoupled and depend on internal nutrient content. The physiological state of an individual at a given time and location thus depends on its life history, i.e. its past physiological state (nutrient quota). Even though Droop and Monod have the same amount of non-linearity, their behaviours are fundamentally different. If we then linearize Droop's model such that:

$$\alpha = F\,\alpha_{\max}\left(\frac{Q}{Q_{\max}}\right) \tag{18}$$

we find that the 2 formulations also give the exact same results (Fig. 2c,d). Apart from verifying the

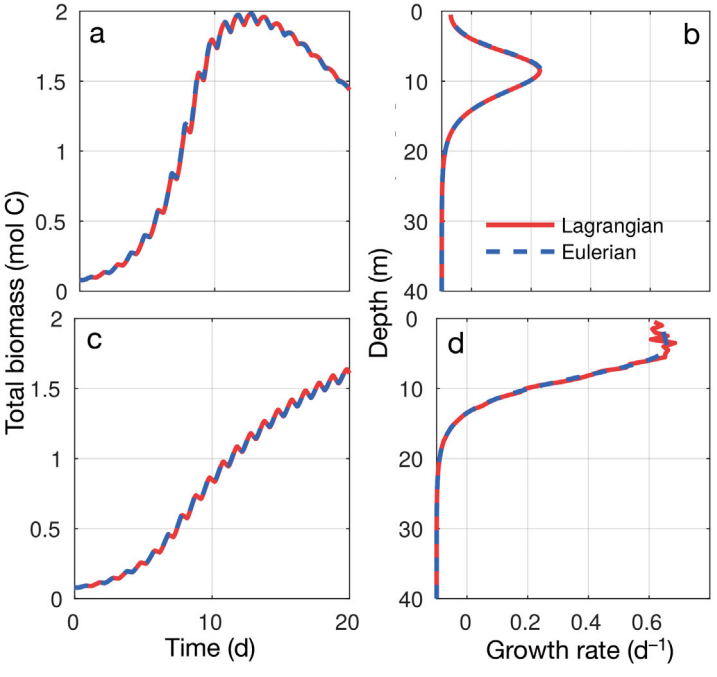

Fig. 2. (a) Total biomass and (b) average growth rate profile at $t = 15$ d obtained with the linearized Monod equation with the Eulerian and Lagrangian formulations. (c) Total biomass and (d) average growth rate profile at $t = 15$ d obtained with the linearized Droop equation

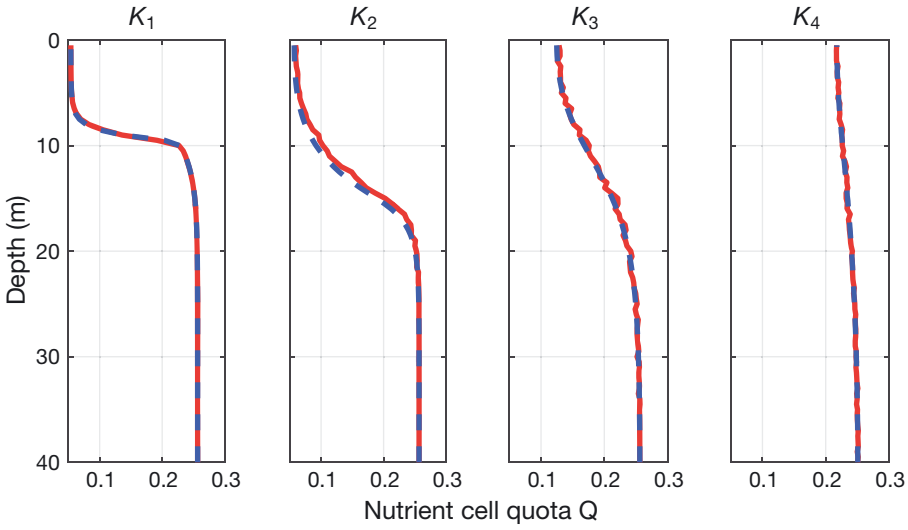

Fig. 3. Instantaneous Eulerian (dashed blue line) and Lagrangian average (solid red line) nutrient cell quota Q profiles at t = 10 d for scenarios K_1 to K_4 (defined in Table 2)

numerical implementation, this result highlights that differences between Eulerian and Lagrangian formulations essentially come from 2 fundamental necessary conditions: (1) particle growth must depend on life history (e.g. internal nutrient concentration) and not only on local conditions (e.g. external nutrient concentration); (2) particle growth must be a nonlinear function of its physiological state, which leads to different behaviour at the population level due to Jensen's inequality.

RESULTS

Cell quota

Snapshots of mean cell quotas after 10 d are presented in Fig. 3 for scenarios K_1–K_4 (Table 2). Due to the consumption of nutrients in the photic zone through photosynthesis, a vertical gradient in the average internal cell quota profile appears (Fig. 3). Note that the Lagrangian profile is noisy as a result of the stochasticity introduced by the random walk. Phytoplankton cells near the surface first consume all external nutrients and then use their internal content until they reach the subsistence quota Q_{min}. At depth, phytoplankton cells incorporate external nutrients until they reach the maximum storage quota Q_{max} without using it for photosynthesis because of the absence of light. This represents a difference in terms of physiological state among the cells in the water column. Because cells at the surface have consumed nutrients for growth (Fig. 4), particles in the upper ocean layer contain a larger amount of cellular carbon but a lower N:C ratio than particles at depth. As turbulent diffusivity increases, this gradient tends to disappear. As mixing increases, a larger fraction of cells coming from the deeper part of the water column where the nutrients are in replete condition are mixed up with those near the surface, contributing to increase the mean cell quota in the upper part of the water column. The same process takes place at depth where cells coming from the upper part are mixed with those from the bottom, leading to a decrease of

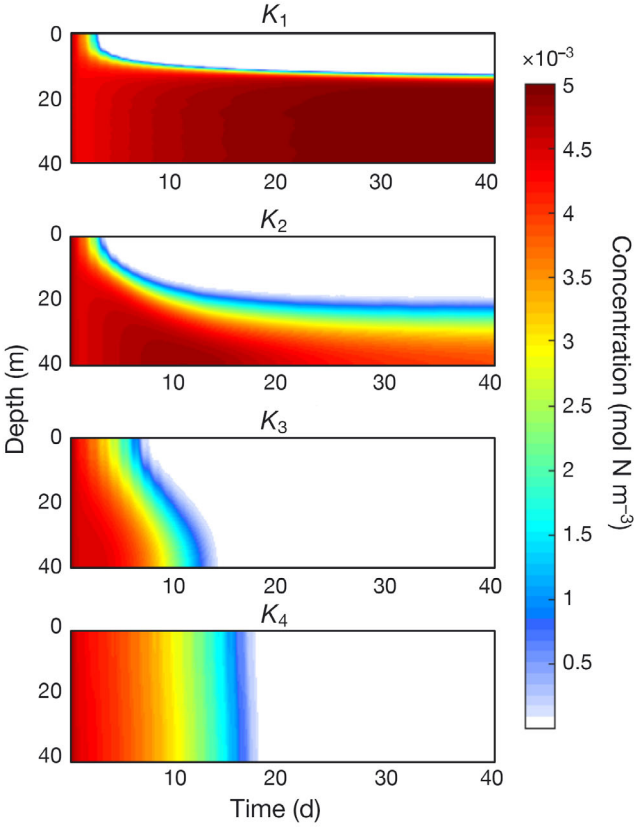

Fig. 4. Evolution of external nutrient concentrations for scenarios K_1 to K_4 (defined in Table 2)

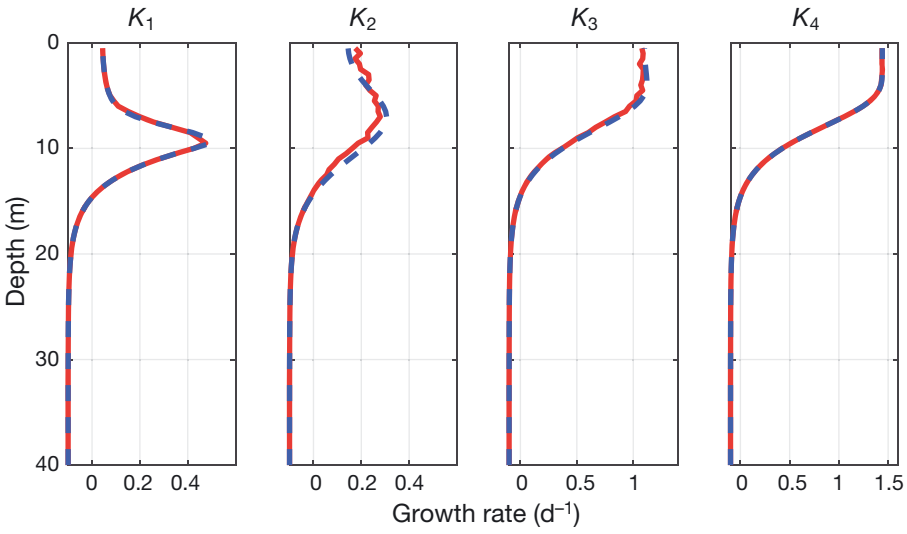

Fig. 5. Instantaneous Eulerian (dashed blue line) and Lagrangian (red solid line) average growth rate profiles at t = 10 d for scenarios K_1 to K_4 (defined in Table 2). Note the different horizontal scales

the mean cell quota in the lower part of the water column. The Eulerian simulations follow the same profile as their Lagrangian counterparts, and no evident difference is noted.

Growth rate

In weak mixing regimes (scenarios K_1 and K_2), a nutrient-depleted condition appears rapidly in the upper layer of the water column, contributing to limit growth rates near the surface at the end of the 10 d simulation (Fig. 5). In the lower part of the water column, light is limiting, preventing phytoplankton growth. The resulting growth rate from nutrient limitation near the surface and light limitation at depth exhibits a maximum at the base of the nutricline. In strong mixing conditions (scenarios K_3 and K_4), nutrients are brought to the surface where light is optimal, sustaining large growth rate values throughout the simulation. The Eulerian formulation sometimes overestimates and sometimes under-estimates growth rates compared to the Lagrangian, depending on the curvature of the non-linear growth function, which itself depends on light and internal cell quota profiles.

Fig. 6 shows the distribution of cell quotas and growth rates of all cells at 5 m below the surface after 10 d. In weak mixing conditions (scenario K_1), the distribution is narrow and both formulations agree in terms of mean values. The same applies to very strong mixing conditions (scenario K_4) where cells are all rapidly moved across varying conditions so that they all experience a similar mean value with little variance. In intermediate mixing conditions, the distributions of internal cell quotas are widespread and non-normal, such that when a non-linear growth function is applied, the result is also non-linear.

To better understand the relation between intra-population variability and the difference between the 2 simulations, snapshots of the distribution of cell quotas and growth rate of all cells at 5 m for scenario K_3 are shown in Fig. 7 at different times of the simulation. At the beginning of the simulation, i.e. before the bloom, nutrients are in replete conditions and all cells have cell quotas close to Q_{max} = 0.25 (molN molC^{-1}). The resulting average growth rate shows no differences between Eulerian and Lagrangian simulations. When external nutrients start to become limiting, mean cell quotas decrease but strong mixing increases the contribution of cells coming from depth with high cell nutrient quotas. Cell quotas are thus widely distributed. Because of the Jensen's inequality, mean growth rates computed by the 2 formulations differ. At the end of the simulation, the water column tends to be homogenized and cell quotas are close to Q_{min}.

Total biomass

The total biomass for scenarios K_1 to K_4 is shown in Fig. 8. Strong mixing allows surface waters to be partially replenished with nutrients, leading to an increase in total biomass in both Eulerian and Lagrangian simulations. Maximum differences between Eulerian and Lagrangian appear at intermediate turbulence values. Although differences in internal cell quotas or in growth rates are not that large, they can contribute to produce large differences in total biomass over the duration of a phytoplankton bloom period or a coastal upwelling event, for example. In

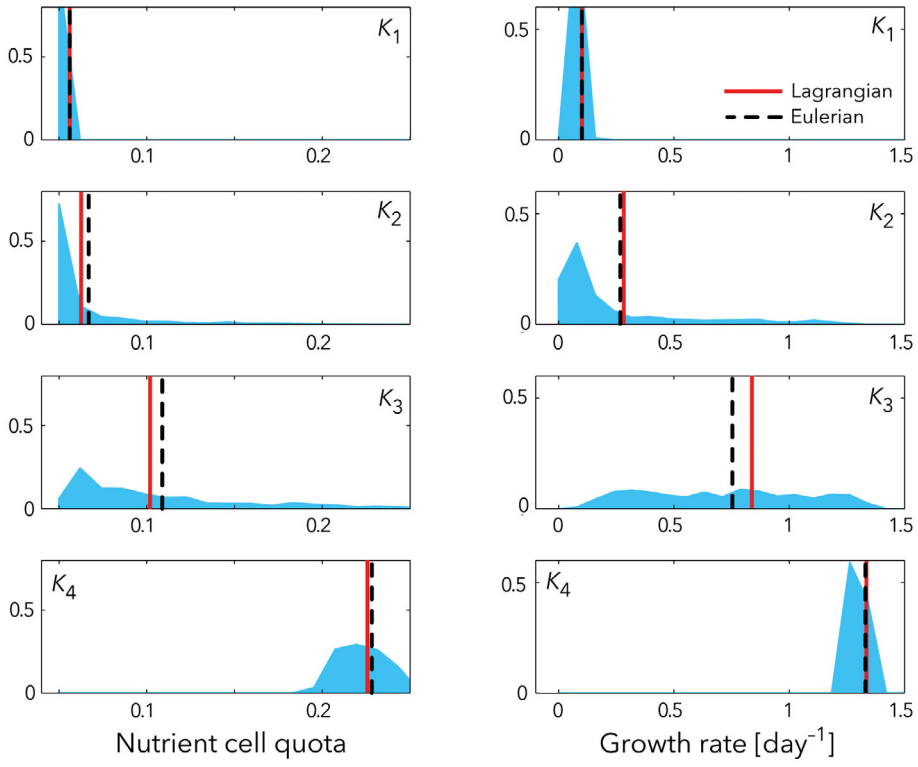

Fig. 6. Intra-population nutrient cell quota (left column) and growth rate (right column) distribution of the Lagrangian model (blue shaded area) at t = 10 d and z = –5 m for scenarios K_1 to K_4 (defined in Table 2). Both Eulerian and Lagrangian mean values are shown

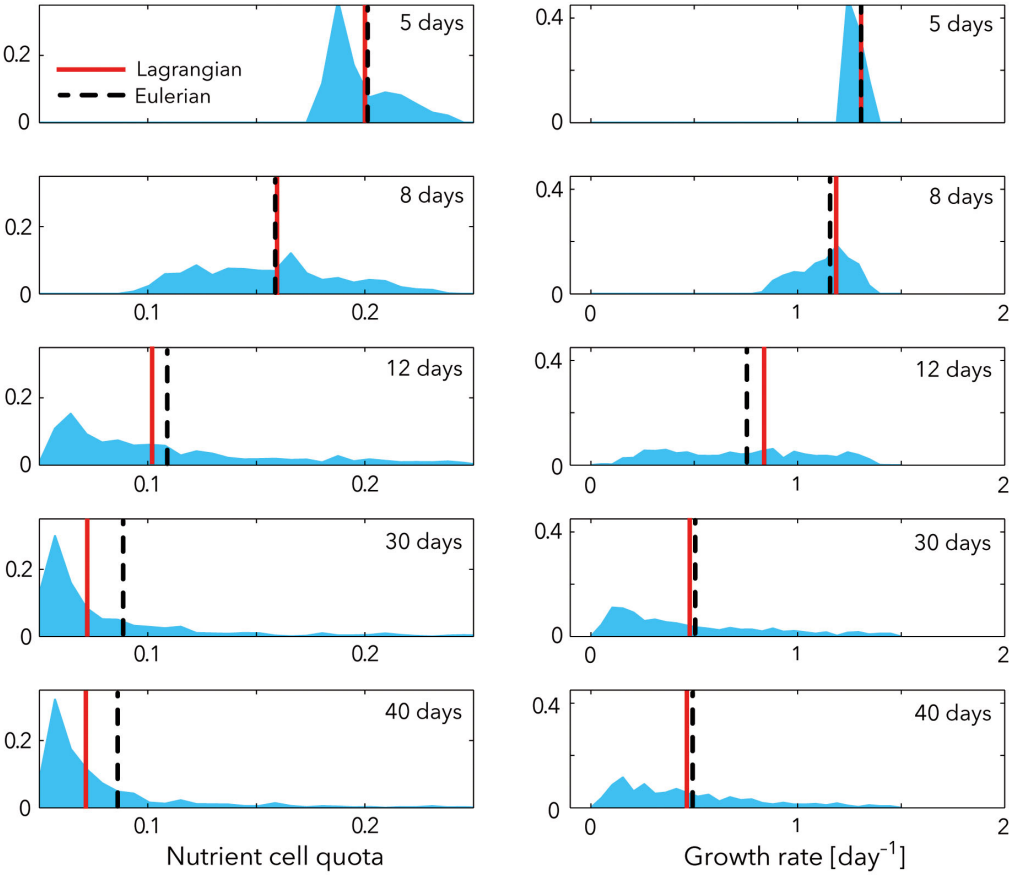

Fig. 7. Intra-population nutrient cell quota (left column) and growth rate (right column) distribution of the Lagrangian model (blue shaded area) at t = 5, 8, 12, 30 and 40 d and z = –5 m for experiment K_3 (defined in Table 2). Both Eulerian and Lagrangian mean values are shown

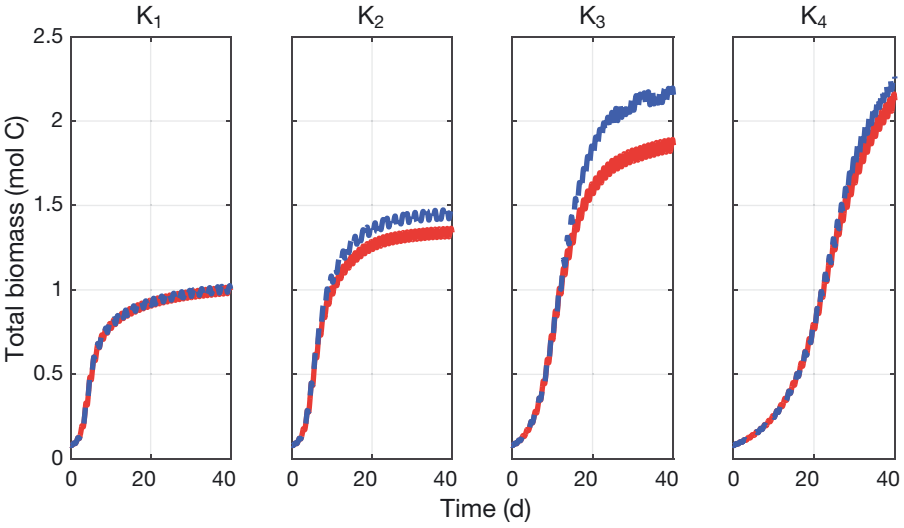

Fig. 8. Evolution of the total biomass obtained from the Eulerian (dashed blue line) and Lagrangian (solid red line) simulations for scenarios K_1–K_4 (defined in Table 2) over 40 d

order to estimate the differences between the 2 formulations in terms of total biomass, we calculated the normalized root mean square error (nRMSE) between Eulerian and Lagrangian formulations for all simulations as a function of time, as:

$$\mathrm{nRMSE}(t) = \left[\frac{\left(\tilde{B}(t) - B(t)\right)^2}{B(t)^2}\right]^{1/2} \times 100\% \qquad (19)$$

where $B(t)$ and $\tilde{B}(t)$ are the total biomass as a function of time in the Eulerian and Lagrangian simulations, respectively. Results for all 7 experiments are shown in Fig. 9. Under realistic mixing conditions such as variable tidal mixing, differences between Eulerian and Lagrangian formulations can reach as much as 10% of the total biomass.

Model sensitivity

In this section, we extend the previous results by investigating the model behaviour in its parameter space. We proceed by analysing the temporal evolution of the error (in terms of biomass), defined here as the difference between the Eulerian and the Lagrangian solutions, for various biological and physical parameter values. The values of phytoplankton growth parameters (i.e. the maximum storage quota Q_{max}, the maximum uptake rate V_{max} and the maximum photosynthesis rate α_{max}) can vary significantly among species and environmental conditions (e.g. in polar versus temperate environments). We thus investigate how different values of these parameters affect the results shown in previous sections. For each parameter, we conducted a set of 20 simulations: 5 parameter values for each of the 4 constant diffusivity scenarios K_1 to K_4, keeping other parameter sets equal to their original values specified in Table 1.

Model sensitivity results in terms of nRMSE (hereafter 'error') growth with time are presented in Figs. 10 & 11. In all cases, the error grows from 0 at the start of the simulation and increases either up to a maximum before slightly decreasing, or up to a saturating value. In some cases, the error grows and returns to 0 before going up again. In all cases, the maximum error is the largest for scenario K_3 (inter-

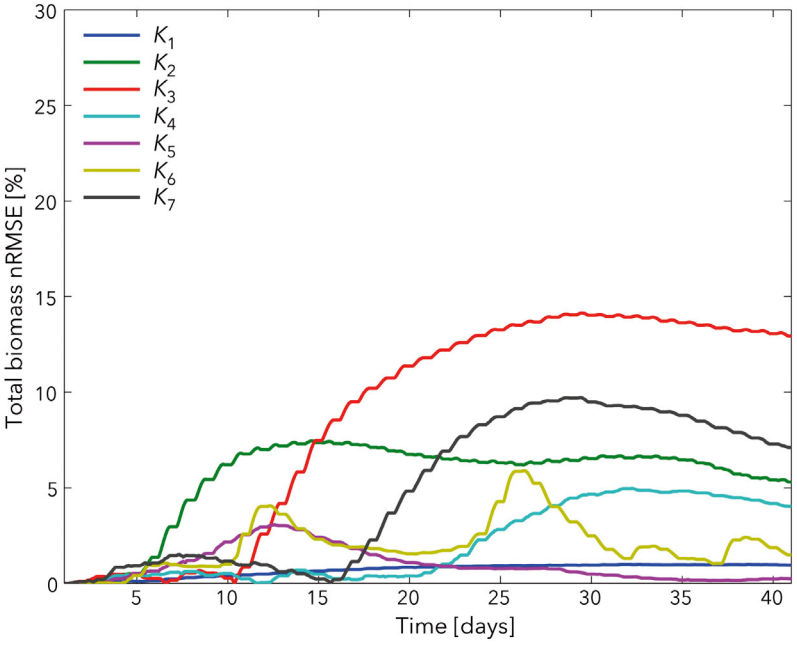

Fig. 9. Normalized root mean square error (nRMSE) of the total biomass as defined by Eq. (16) for all mixing scenarios defined in Table 2

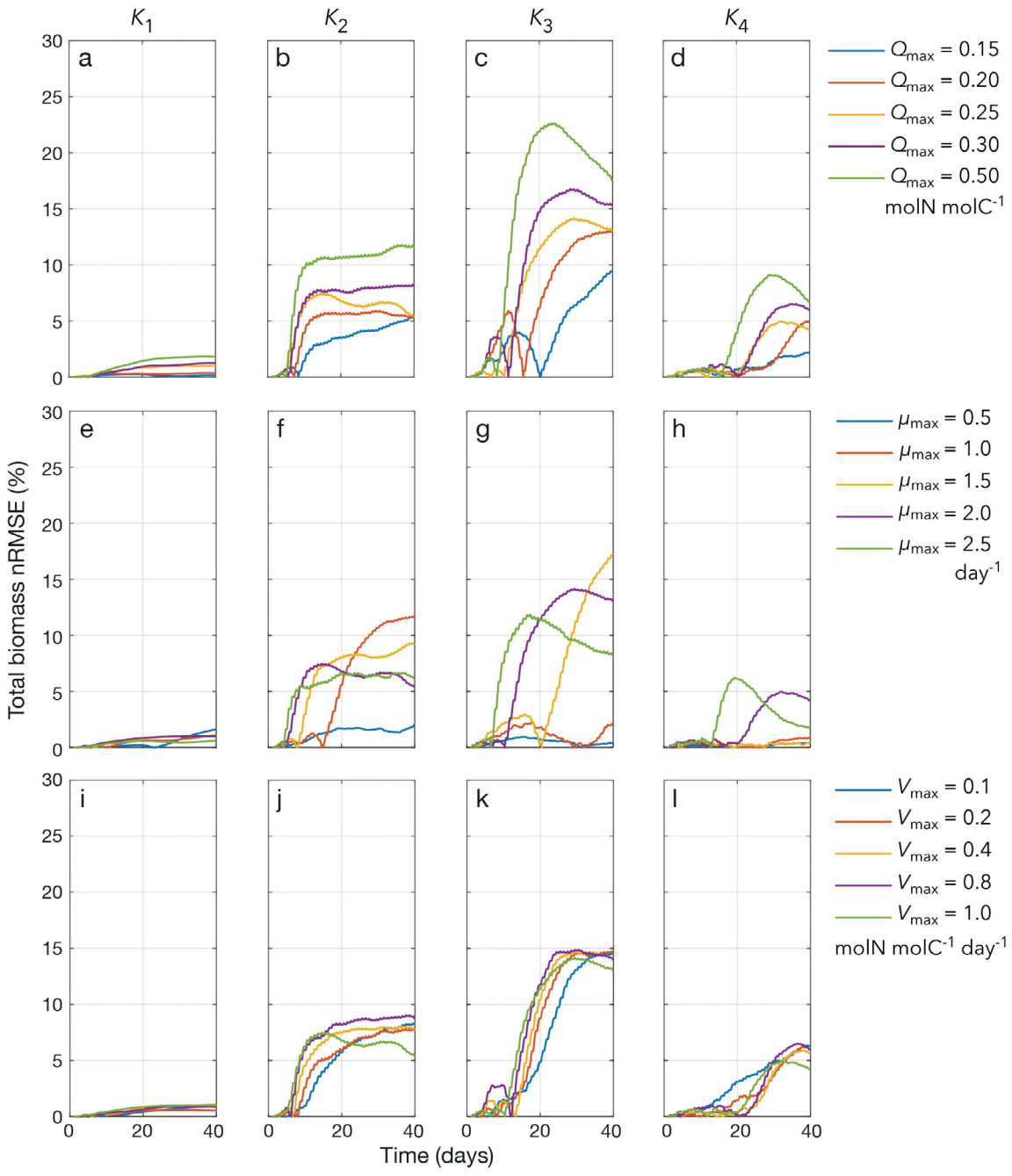

Fig. 10. Normalized root mean square error (nRMSE) of the total biomass as defined by Eq. (16) for scenarios K_1 to K_4 (defined in Table 2) obtained with: (a–d) maximum storage quota values Q_{max} of 0.15, 0.2, 0.25, 0.3 and 0.5 molN molC^{-1}; (e–h) maximum growth rate values μ_{max} = 0.5, 1.0, 1.5, 2.0 and 2.5 d^{-1}; (i–l) maximum nutrient uptake rate values V_{max} = 0.1, 0.2, 0.4 and 0.8 molN molC^{-1} d^{-1}

mediate-strong mixing, 10–20%), and the smallest for scenario K_1 (very weak mixing, <2%).

The error is highly dependent on Q_{max} in the sense that for each mixing scenario and particularly for intermediate diffusivity levels (Fig. 10b,c), the error increases with Q_{max}. This result is consistent with the fact that a higher Q_{max} allows for higher intra-population variability — the higher the value of Q_{max} the larger the range of internal nutrient content that a single cell can carry — and thus increases the potential for discrepancies caused by Jensen's inequality. On the other hand, changing the maximum nutri-

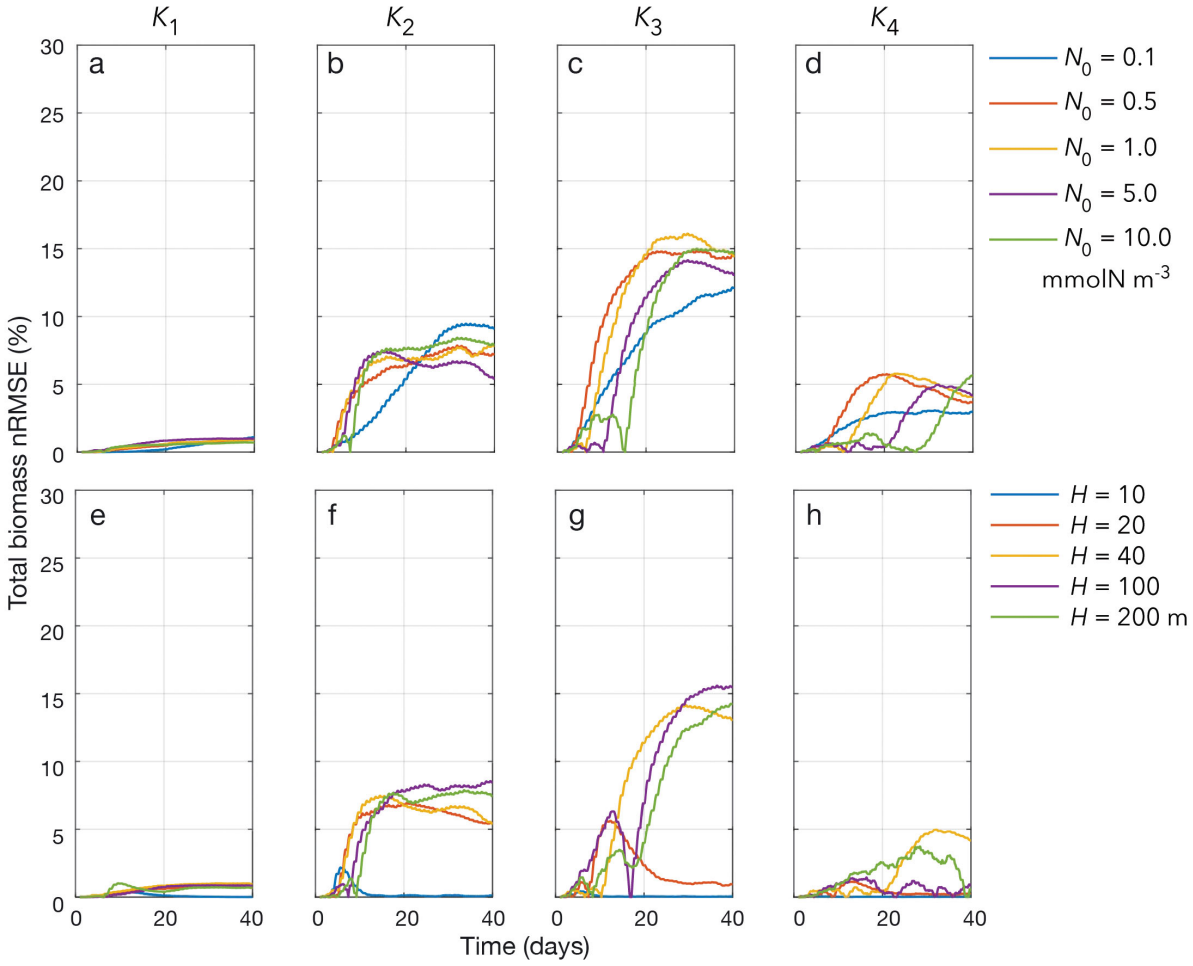

Fig. 11. Normalized root mean square error (nRMSE) of the total biomass as defined by Eq. (16) for scenarios K_1 to K_4 (defined in Table 2) obtained with: (a–d) initial nutrient concentrations values N_0 = 0.1, 0.5, 1.0, 5.0 and 10.0 mmolN m^{-3}; (e–h) depth values H = 10, 20, 40, 100 and 200 m

ent uptake rate V_{max} has less impact on the error (Fig. 10i–l).

In order to investigate the effect of the maximum growth rate, we chose values ranging from 0.5 to 2.5 d^{-1} (Fig. 10e–h). This parameter is the most likely to differ between species and environmental conditions in nature. Its effect on the error is significant both in terms of amplitude and the time evolution at which the 2 formulations start to diverge. This behaviour highlights that the development of intra-population variability depends on the relationship between growth and mixing and time scales. To illustrate this, let $\tau_K = \Delta z^2/K$ be the time taken by a cell to travel through a distance Δz due to a diffusivity K and let $\tau_g = 1/\alpha$ be the time taken for cells to significantly grow. In the limit where $\tau_K \ll \tau_g$, cells are randomly transported across the water column more rapidly that they can divide. All cells are thus exposed to practically the same rapidly changing environmental conditions, and thus grow at similar rates, and intra-population variability is low and both formulations provide similar results. In contrast, if $\tau_K \gg \tau_g$, cells living at a particular depth in the water column are exposed to very similar environmental conditions and divide more rapidly than they are brought apart by turbulent motion. Consequently, the intra-population variability is also minimized and both formulations provide similar results. When $\tau_K \sim \tau_g$, cells grow over at the same rate as they are brought apart from each other, thus experiencing different life histories. In these conditions, the error is more likely to be important (see for instance Fig. 10, for K_2, K_3 and K_4).

Since the discrepancy between the 2 formulations is directly constrained by the presence of environmental gradients, we also investigated how the depth of the water column and the initial nutrient concen-

tration affect the results. For this analysis, we chose 5 depth values ranging from very shallow waters (10 m) to deeper waters (200 m), representative of coastal ecosystems. Results are presented in Fig. 11. For 10 m deep water columns, the error between Eulerian and Lagrangian simulations is very close to 0 for all turbulent regimes. In this case, the water column is shallower than the photic zone (ca. ~11 m), leading to a similar consumption rate of nutrients between the surface and the sea bed. For 20 m depth and scenario K_3 (Fig. 11g), the error increases during the first few days of the simulations and decreases rapidly after the water column has been completely homogenized due to mixing. For deeper waters, the error behaves in a similar fashion.

For assessing the error sensitivity to initial nutrient concentrations N_0, we chose 5 values ranging from oligotrophic conditions (0.1 to 1.0 mmolN m^{-3}) to eutrophic conditions (5 and 10 mmolN m^{-3}). The half-saturation constant for nutrient uptake is k_n = 0.214 mmolN m^{-3}. As expected, varying the initial nutrient concentration mainly affects the timing at which the results from the 2 formulations start to diverge, which corresponds to the time needed to produce vertical gradients of nutrient uptake and cell growth. In oligotrophic conditions, gradients appear rapidly and lead to an early increase of the error. However, in eutrophic conditions, the error starts to increase only after 15 or 20 d (scenario K_4).

DISCUSSION AND CONCLUSION

In this paper, we addressed the question of the role of turbulent mixing in producing and altering intra-population variability in terms of nutrient cell quota and how it impacts the discrepancies between Lagrangian and Eulerian formulations in a 1-dimensional water column model.

First, our experiments showed that the Eulerian model systematically overestimated (if not equalled) the phytoplankton biomass compared to the Lagrangian approach, which is a consequence of Jensen's inequality. This result is not new, and numerous modelling studies applied to wastewater treatment plants have reported it (e.g. Gujer 2002, Schuler 2005). For instance, Bucci et al. (2012) studied variability in terms of phosphate cell quota in enhanced biological phosphorus removal and showed that the Eulerian model can produce approximately the same results as the Lagrangian version only if the value of the growth rate is reduced by 55%. In a similar experiment, Fredrick et al. (2013) showed that the Eulerian formulation overestimates biomass by >40%. It is noticeable that in these studies, differences among individuals emerged from phenotypical variability introduced explicitly in the Lagrangian model by randomizing cell parameters during cell division.

Other studies have provided a comparison between Lagrangian and Eulerian approaches in natural environments, exploring the variability in terms of nutrient cell quota induced by different life histories. Broekhuizen et al. (2003) used a 3-dimensional Lagrangian model ensemble applied to a shelf sea area in New Zealand. The model included multi-nutrient consumption, photosynthesis with a Droop-type formulation, many different phytoplankton species and swimming strategies. They showed that variability in terms of individual nitrate cell quota of diatoms was particularly strong in areas with strong nitrate gradients and produced differences of up to 30% of the biomass between the 2 formulations. While the magnitude of the difference is similar to our results, they showed that the Eulerian formulation does not systematically overestimate the biomass, but instead often produced lower results. As they mentioned, this result emerges from the sigmoid form they used for the Droop-type equation of photosynthesis since for small cell quotas, the function has a concave form. According to Jensen's inequality, the Eulerian formulation will overestimate (underestimate) its Lagrangian counterpart if the non-linear function is convex (concave).

Second, we showed that in marine environments, the mixing regime strongly controls the variability among individuals and therefore the discrepancy between the results of the Lagrangian and the Eulerian approaches. The first set of idealized experiments using uniform and constant diffusivity profiles ranging from 10^{-6} to 10^{-2} m^2 s^{-1} highlighted that the maximum variability among individuals corresponds to cases when turbulent mixing is strong enough to transport cells through the water column, but sufficiently low to maintain a certain stratification in the external nutrient content. It is important to note that, in our experiments, nutrient stratification was only caused by phytoplankton consumption in the surface layer. However, nutricline layers are observed in moderate to strong vertical mixing conditions, e.g. in estuarine or frontal systems. In the context of phytoplankton growth, it is therefore important to make the distinction between 'mixing' layer and 'mixed' layer (Taylor & Ferrari 2011), the first referring to a layer where turbulent mixing is strong and the latter referring to a layer that is homogenized but in which

active mixing is not necessarily happening. In the first case, intra-population variability can be large if stratification persists as cells are transported rapidly through different environments. In the latter, all cells experience the same environmental conditions and intra-population variability is minimized.

The sensitivity analysis revealed that the magnitude of the error is very sensitive to the maximum nitrate storage quota Q_{max}, which plays a key role in controlling the range of internal nitrate that an individual cell can carry and therefore modulates the variability between individuals. This result is consistent with Fredrick et al. (2013), who explored the relative contribution of several biological parameters to intra-population variability in terms of the internal phosphorus content of the planktonic diatom *Thalassiosira pseudonana*. They found that the variability of Q_{max} was the main factor influencing intra-population heterogeneity, in agreement with our results.

The maximum growth rate value also influences Eulerian versus Lagrangian discrepancies mostly because of its relation with the mixing time scale. The largest errors occur when the mixing rate and the growth rate are of the same order of magnitude. We have also shown that Eulerian and Lagrangian formulations give significantly different results under realistic conditions such as wind-induced and tidal mixing. An interesting observable feature in wind-induced mixing experiments is the non-monotonic behaviour of the error: during strong wind events, cells can be rapidly transported in the water column on short time scales, enhancing intra-population heterogeneity. After these events, the error between Lagrangian and Eulerian formulations is thus temporally higher, although it can decrease when stratification is restored.

The only source of intra-population heterogeneity we considered in our study is the internal nutrient cell quota carried by each individual. However, in real environments, numerous other complex physiological mechanisms are responsible for introducing variability between individuals, and each of these processes and their impact on the population behaviour are not always the same.

One example is photo-acclimation. As cells are transported through the water column, they experience many different light conditions and are able to acclimate by adjusting their physiological response to ambient light (i.e. changing their chlorophyll to carbon ratio) (Falkowski & LaRoche 1991, Geider et al. 1997, MacIntyre et al. 2002). If mixing is weak, the time scale of vertical transport is less than the photoresponse time scale and cells can thus acclimate. As a result, the population at a given depth is composed of many individuals with different photosynthetic capacities inherited from their life histories. However, if mixing is strong, phytoplankton cells do not have enough time to adjust their response to a changing environment, keeping intra-population heterogeneity to a minimum. There is also, in this case, a clear connection between mixing and heterogeneity. However, in contrast to our study, light is not physically mixable as nutrients are; light only affects growth time scales and this might affect the contrast between Eulerian and Lagrangian simulations. For instance, Lande & Lewis (1989) found no significant differences in photosynthetic rates between the 2 approaches (<1%) for diffusivity of 0.01 m^2 s^{-1}. McGillicuddy (1995) showed that the 2 formulations produced more differences when the photo-acclimation model of Wolf & Woods (1988) was applied for the same mixing regimes. This discrepancy with the findings of Lande & Lewis (1989) was attributed to the different photoresponse time scales used in the 2 studies.

New generations of models take into account several sources of heterogeneity and simulate Droop's kinetics, photo-acclimation (Ross & Geider 2009), multi-nutrient limitations and several other factors. Adding more processes has a potential to further increase the error in Eulerian models and lead to misinterpretations of model results. It is thus fundamental for modellers to inquire about these questions, i.e. the processes to be studied as well as the physical environment one wants to simulate, before choosing a numerical formulation, Eulerian or Lagrangian.

Acknowledgements. We thank Oliver Ross for providing several parts of the code, Ferdi Hellweger for guidance and help, Frédéric Maps and Gustavo Ferreyra for useful feedback, and 2 anonymous reviewers whose comments contributed to increasing the quality of the text. This research was funded by NSERC Discovery Grant No. 402257-2013 to D.D. and the FRQNT Québec-Océan Strategic cluster. A documented Fortran version of the model is available in open access from the following GitLab repository: https://gitlasso.uqar.ca/dumoda01/phlag.git.

LITERATURE CITED

Arhonditsis GB, Brett MT (2004) Evaluation of the current state of mechanistic aquatic biogeochemical modeling. Mar Ecol Prog Ser 271:13–26

Baklouti M, Diaz F, Pinazo C, Faure V, Quéguiner B (2006) Investigation of mechanistic formulations depicting phytoplankton dynamics for models of marine pelagic ecosystems and descriptions of a new model. Prog Oceanogr

71:1–33
Bolnick DI, Amarasekare P, Araújo MS, Bürger R and others (2011) Why intraspecific trait variation matters in community ecology. Trends Ecol Evol 26:183–192
Brand L, Guillard R (1981) The effects of continuous light and light intensity on the reproduction rates of twenty-two species of marine phytoplankton. J Exp Mar Biol Ecol 50:119–132
Broekhuizen N (1999) Simulating motile algae using a mixed Eulerian-Lagrangian approach: Does motility promote dinoflagellate persistence or co-existence with diatoms? J Plankton Res 21:1191–1216
Broekhuizen N, Oldmam J, Zeldis J (2003) Sub-grid-scale differences between individuals influence simulated phytoplankton production and biomass in a shelf-sea system. Mar Ecol Prog Ser 252:61–76
Bucci V, Majed N, Hellweger FL, Gu AZ (2012) Heterogeneity of intracellular polymer storage states in enhanced biological phosphorus removal (EBPR)–observation and modeling. Environ Sci Technol 46:3244–3252
Cianelli D, Sabia L, d'Alcal'a MR, Zambianchi E (2009) An individual-based analysis of the dynamics of two coexisting phytoplankton species in the mixed layer. Ecol Model 220:2380–2392
Cianelli D, Uttieri M, Zambianchi E (2012) Individual based modelling of planktonic organisms. In: Zhang W (ed) Ecological modeling. Nova Science Publisher, New York, NY, p 83–96
Cullen J, Lewis M (1988) The kinetics of algal photoadaptation in the context of vertical mixing. J Plankton Res 10: 1039–1063
Dortch Q, Maske H (1982) Dark uptake of nitrate and nitrate reductase activity of a red-tide population off Peru. Mar Ecol Prog Ser 9:299–303
Droop M (1974) The nutrient status of algal cells in continuous culture. J Mar Biol Assoc UK 54:825–855
Esposito S, Botte V, Iudicone D, d'Alcala MR (2009) Numerical analysis of cumulative impact of phytoplankton photoresponses to light variation on carbon assimilation. J Theor Biol 261:361–371
Falkowski P, LaRoche J (1991) Minireview: Acclimation to spectral irradiance in algae. J Phycol 27:8–14
Franks PJ (2002) NPZ models of plankton dynamics: their construction, coupling to physics, and application. J Oceanogr 58:379–387
Fredrick ND, Berges JA, Twining BS, Nuñez-Milland D, Hellweger FL (2013) Use of agent-based modeling to explore the mechanisms of intracellular phosphorus heterogeneity in cultured phytoplankton. Appl Environ Microbiol 79:4359–4368
Geider RJ, MacIntyre HL, Kana TM (1997) Dynamic model of phytoplankton growth and acclimation: responses of the balanced growth rate and the chlorophyll *a*:carbon ratio to light, nutrient-limitation and temperature. Mar Ecol Prog Ser 148:187–200
Graham DI, Moyeed RA (2002) How many particles for my Lagrangian simulations? Powder Technol 125:179–186
Grimm V, Berger U, Bastiansen F, Eliassen S and others (2006) A standard protocol for describing individual-based and agent-based models. Ecol Model 198:115–126
Gujer W (2002) Microscopic versus macroscopic biomass models in activated sludge systems. Water Sci Tech 45: 1–11
Hellweger FL, Bucci V (2009) A bunch of tiny individuals — individual-based modeling for microbes. Ecol Model 220: 8–22
Hellweger FL, Kianirad E (2007) Accounting for intrapopulation variability in biogeochemical models using agent-based methods. Environ Sci Technol 41:2855–2860
Huisman J, Sharples J, Stroom JM, Visser PM, Kaardinal WEA, Verspagen JMH, Sommeijer B (2004) Changes in turbulent mixing shift competition for light between phytoplankton species. Ecology 85:2960–2970
Hunter J, Craig P, Phillips H (1993) On the use of random walk models with spatially variable diffusivity. J Comput Phys 106:366–376
Jensen JLWV (1906) Sur les fonctions convexes et les inégalités entre les valeurs moyennes. Acta Math 30:175–193
Kamykowski D, Yamazaki H, Janowitz GS (1994) A Lagrangian model of phytoplankton photosynthetic response in the upper mixed layer. J Plankton Res 16: 1059–1069
Lande R, Lewis M (1989) Models of photoadaptation and photosynthesis by algal cells in a turbulent mixed layer. Deep-Sea Res 36:1161–1175
Large WG, McWilliams JC (1994) Oceanic vertical mixing: a review and a model with a nonlocal boundary layer parameterization. Rev Geophys 32:363–403
MacIntyre HL, Kana TM, Anning J, Geider RJ (2002) Photoacclimation of photosynthesis irradiance response curves and photosynthetic pigments in microalgae and cyanobacteria. J Phycol 38:17–38
McGillicuddy D (1995) One dimensional numerical simulation of primary production: Lagrangian and Eulerian formulation. J Plankton Res 17:405–412
Nagai T, Yamazaki H, Kamykowski D (2003) A Lagrangian photoresponse model coupled with 2nd-order turbulence closure. Mar Ecol Prog Ser 265:17–30
Ross ON, Geider RJ (2009) New cell-based model of photosynthesis and photo-acclimation: accumulation and mobilisation of energy reserves in phytoplankton. Mar Ecol Prog Ser 383:53–71
Ross ON, Sharples J (2004) Recipe for 1-D Lagrangian particle tracking models in space-varying diffusivity. Limnol Oceanogr Methods 2:289–302
Ross ON, Sharples J (2007) Phytoplankton motility and the competition for nutrients in the thermocline. Mar Ecol Prog Ser 347:21–38
Ross ON, Sharples J (2008) Swimming for survival: a role of phytoplankton motility in a stratified turbulent environment. J Mar Syst 70:248–262
Ross ON, Geider RJ, Berdalet E, Artigas ML, Piera J (2011) Modelling the effect of vertical mixing on bottle incubations for determining *in situ* phytoplankton dynamics. I. Growth rates. Mar Ecol Prog Ser 435:13–31
Schuler AJ (2005) Diversity matters: dynamic simulation of distributed bacterial states in suspended growth biological wastewater treatment systems. Biotechnol Bioeng 91:62–74
Sharples J (1999) Investigating the seasonal vertical structure of phytoplankton in shelf seas. Mar Models 1:3–38
Taylor JR, Ferrari R (2011) Shutdown of turbulent convection as a new criterion for the onset of spring phytoplankton blooms. Limnol Oceanogr 56:2293–2307
Umlauf L, Burchard H (2005) Second-order turbulence closure models for geophysical boundary layers. A review of recent work. Cont Shelf Res 25:795–827
Visser AW (1997) Using random walk models to simulate the

vertical distribution of particles in a turbulent water column. Mar Ecol Prog Ser 158:275–281

Wolf KU, Woods JD (1988) Lagrangian simulation of primary production in the physical environment — the deep chlorophyll maximum and nutricline. In: Rothschild BJ (ed) Toward a theory on biological-physical interactions in the World ocean. NATO ASI Series (Series C: Mathematical and Physical Sciences), Vol 239. Springer, Dordrecht, p 51–70

Woods JD, Onken R (1982) Diurnal variation and primary production in the ocean: preliminary results of a Lagrangian ensemble model. J Plankton Res 4:735–756

Editorial responsibility: Steven Lohrenz, New Bedford, Massachusetts, USA

Submitted: August 29, 2017; Accepted: May 9, 2018
Proofs received from author(s): July 6, 2018